Electro-Optical Properties of Waveguides Based on a Main-Chain Nonlinear Optical Polyamide

Oscar Ahumada, Christoph Weder, Peter Neuenschwander, and Ulrich W. Suter*

Department of Materials, Institute of Polymers, ETH, CH-8092 Zürich, Switzerland

Stephan Herminghaus

Max-Planck-Institut für Kolloid- und Grenzflächenforschung, D-12489 Berlin, Germany

Received December 26, 1996; Revised Manuscript Received March 20, 1997[⊗]

ABSTRACT: Polyamides based on 2′,5′-diamino-4-(dimethylamino)-4′-nitrostilbene (DDANS) and linear aliphatic diacids represent a class of polymers with large and stable second-order nonlinear optical properties, where the nonlinear optical units are fixed in the polymer backbone with their dipole moments oriented transversely to the main chain. Such NLO polymers were processed by spin-coating into planar waveguides ranging from 500 to 1500 nm in thickness. Subsequently, a macroscopic noncentrosymmetric orientation of the NLO-phores was induced by a corona-discharge poling process. The refractive indices, n_{TM} and n_{TE}, and the electro-optic coefficients, r_{33} and r_{13}, were determined by measurement of the waveguiding modes of such devices at a wavelength of 785 nm. The electro-optic coefficient r_{33} of 12 pm/V compares favorably with state-of-the-art polymeric electro-optic materials. It also equals approximately the electronic contribution to the electro-optic effect which can be calculated from the nonlinear optical susceptibility d_{33}. The ratio of electro-optic coefficients r_{33}/r_{31} was found to be ≈3, independent of the magnitude of the NLO-phore orientation. This behavior is in perfect agreement with the predictions from the *isotropic model*.

I. Introduction

In recent years there has been considerable interest in nonlinear optical (NLO) and electro-optic (EO) polymers because of their potential application in efficient, ultrafast, and low-voltage integrated electro-optical devices.[1] The frequently cited advantages of poled polymers are large nonlinear susceptibilities and EO coefficients, fast response times, and easy processability. However, additional requirements such as long-term stability of the NLO or EO effect, high physical and chemical stability, and low optical propagation losses must be satisfied before polymeric materials can demonstrate their potential as actual device materials.[1]

Recently, we have developed a new approach to the design of NLO polymers with large and stable second-order nonlinear susceptibilities.[2−6] In these polymers, the NLO-phores are part of the polymer backbone with their major dipole moment oriented transversely to the polymer main chain. This structure is a consequence of the assumption that in this arrangement the NLO-phores can easily be oriented above their glass transition by an external electrical field but exhibit an improved orientational stability below T_g, when compared to guest−host or side-chain NLO polymers. Within the framework of this concept, we have reported the preparation of a series of semiflexible polyamides based on the bifunctional NLO-phore 2′,5′-diamino-4-(dimethyamino)-4′-nitrostilbene (DDANS) and different linear aliphatic diacid chlorides (Figure 1 contains the polymer example relevant here).[2] The polymers are amorphous, showing glass transition temperatures that depend on the number of methylene groups of the diacid chloride and range from 125 up to 206 °C. Transparent thin films of these polymers can easily be oriented by a corona-discharge poling process. Indeed, large second-order nonlinear optical coefficients (d_{33}) of up to 40 pm/V at a fundamental wavelength of 1542 nm and electronic electro-optical coefficients (r_{33}) of up to 16 pm/V (1300 nm) have been determined, using a standard Maker-fringe technique.[2] Orientational relaxation experiments have revealed a remarkable orientational stability for these polymers.[3] At ambient conditions, no significant relaxation of the NLO coefficients can be observed within 240 days after poling in any of these polymeric materials. Also at elevated temperatures, these new polyamides exhibit an enhanced orientational stability, as can be seen from the aging data.

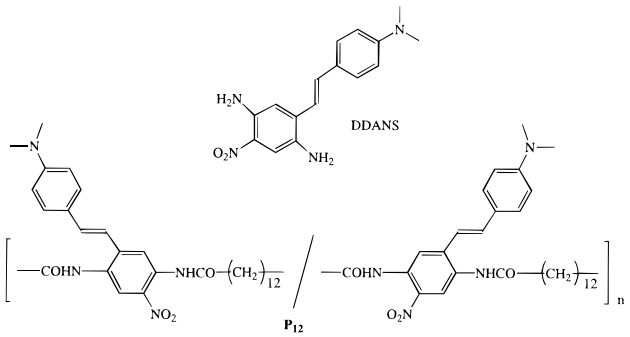

Figure 1. DDANS and the aromatic-aliphatic NLO polyamide $\mathbf{P_{12}}$ under investigation.

In order to demonstrate the usefulness of these new NLO polyamides in actual devices, the electro-optical properties of planar waveguides from one of the polymers of the series, $\mathbf{P_{12}}$ (see Figure 1), are investigated here by measurements of the waveguiding modes relevant for such devices, using attenuated-total-reflectance (ATR) spectroscopy.[7−9] The electro-optic coefficients so determined are compared with the electronic contribution to the electro-optic effect that has been calculated from the nonlinear optical susceptibility, and the ratio of electro-optic coefficients r_{33} and r_{13} is discussed with respect to the predictions that are derived from the isotropic model.[10]

[⊗] Abstract published in *Advance ACS Abstracts,* May 1, 1997.

S0024-9297(96)01898-0 CCC: $14.00

II. Theory

Isotropic Model. The macroscopic noncentrosymmetric orientation of the NLO-phores, which is a prerequisite for second-order NLO effects, is generally achieved by poling the material in an electrical field.[1] In this process, the temperature of the polymer film is raised to near its glass transition temperature while a dc electric field is applied. Thus, the permanent dipoles of the NLO-phores experience a force, tending to align them in the direction of the field. If the equilibrium is established, the net orientation is determined by the potential energy of the molecular dipoles in the applied field relative to the energy associated with thermal fluctuations of the system, as well as the dielectric and electric properties of the medium and its interfaces.[11] The system is then cooled under the influence of the poling field and the alignment of the NLO-phores is retained in the glassy state.

This poling process is conceptually simple, but the related complex physical processes are quite difficult to express theoretically. The *isotropic model* is the most common way to describe the effects of poling in a polymeric NLO material.[10−13] The main assumptions made by this model can be summarized as follows:[11] The NLO-phores in an isotropic polymer matrix are treated as independent particles, the interactions of which (among themselves and with the polymeric host) are not influenced by the orientation of the system, which in turn is induced by the poling process only. Since the average orientation of the NLO-phores in a polymer so induced is typically small (order parameters of 0.3 for $\cos^3 \alpha$ are often quoted,[14,15] with α defined as the average angle between the NLO-phore's molecular axis and the poling direction), this approximation holds generally well for amorphous polymers.

Using the approximations of the *isotropic model* as discussed above, assuming that the NLO-phore's static dipole moment μ is parallel to the NLO-phore's molecular axis chosen to define α and that the internal electric field $\boldsymbol{F}$ is parallel to the poling field, the average value of $\cos^n \alpha$ at equilibrium becomes[10]

$$\langle \cos^n \alpha \rangle = \frac{\int_0^\pi \exp[-\mu F \cos \alpha / kT] \cos^n \alpha \sin \alpha \, d\alpha}{\int_0^\pi \exp[-\mu F \cos \alpha / kT] \sin \alpha \, d\alpha} \quad (1)$$

where μ and F are the magnitudes of the respectives vectors. The solutions of eq 1 are the Langevin functions. The relevant ones for this model are $L_1(u)$ and $L_3(u)$, which, respectively, relate to $\cos \alpha$ and $\cos^3 \alpha$, defining $u = \mu F/kT$ as the poling parameter. For the regime where the poling energy is smaller than the thermal energy of the NLO-phore ($u \leq 1$), the Langevin functions reduce to[10,16]

$$L_1(u) \approx \frac{u}{3} \quad (2)$$

and

$$L_3(u) \approx \frac{u}{5} \quad (3)$$

The macroscopic second-order nonlinear properties of a poled polymer are characterized by the nonlinear optical susceptibility $\chi^{(2)}_{IJK}(-\omega;\omega_1,\omega_2)$. The simple model of noninteracting NLO-phores[17] relates this susceptibility tensor to the NLO-phore's molecular hyperpolarizability β_{IJK}, the number density of the NLO-phores, and the local field factors in the Lorentz approximation f ($f = (n^2 + 2)/3$). Taking Kleinmann symmetry[18] into account, the susceptibility tensor is completely defined by the susceptibility in the direction z of the poling field:

$$\chi^{(2)}_{333}(-\omega;\omega_1,\omega_2) = N f_\omega f_{\omega_1} f_{\omega_2} \beta_{zzz} \langle \cos^3 \alpha \rangle \quad (4)$$

and the susceptibility perpendicular to the poling direction:

$$\chi^{(2)}_{113}(-\omega;\omega_1,\omega_2) = N f_\omega f_{\omega_1} f_{\omega_2} \beta_{zzz} \frac{1}{2} [\langle \cos \alpha \rangle - \langle \cos^3 \alpha \rangle] \quad (5)$$

Usually, these tensor components are simply referred to as χ_{33} and χ_{31}. They are related to the nonlinear optical coefficients d_{33} and d_{31} by a factor of 2 and, as discussed below, are also directly related to the electro-optic coefficients r_{33} and r_{31}.

Using the average $\langle \cos^n \alpha \rangle$ (eq 1) and utilizing the simplified Langevin functions for small values of the argument u, eqs 4 and 5 reveal that the ratios χ_{33}/χ_{31}, d_{33}/d_{13}, and r_{33}/r_{13} all equal the value 3:

$$\frac{\chi_{33}}{\chi_{13}} = \frac{d_{33}}{d_{13}} = \frac{r_{33}}{r_{13}} \approx 3 \quad (6)$$

In many cases where both tensor components of either the NLO or the EO coefficients have independently been measured, the ratio 3 predicted by the isotropic model is in good agreement with the experimental data.[19−23] However, substantial deviations from this isotropic behavior have sometimes been observed.[7,24,25] Such deviations can have a variety of origins all deriving from situations where one or more of the approximations made within the frame of the above discussed model are violated. Typical situations include poling at high field strength,[26] strong interactions between the NLO-phores, such as in liquid crystalline phases,[27] or photophysical experiments carried out at optical frequencies near the NLO-phores' resonance.[28] It has also been shown[7] that higher ratios can arise as well if the mobility of the NLO-phores is significantly restricted by their immediate environment. Within this concept, a threshold torque is required before a dipole can be oriented and this threshold may be different for different NLO-phores.

Relation between NLO and EO Coefficients. The electro-optic coefficient r_{ijk} is the sum of an electronic contribution (r^e_{ijk}) and the effects from optic (r^o_{ijk}) and acoustic (r^a_{ijk}) phonons. The electro-optic effect for organic materials is assumed to be mainly of *electronic* origin.[29] There exists, therefore, a direct relation between *electronic* EO and NLO coefficients:[30]

$$r^e_{ijk} = \frac{-4}{n_i^2 n_j^2} d^{EO}_{ijk} \quad (7)$$

where the nonlinear optical coefficient d^{EO}_{ijk} for a static and an optical field at frequency ω is related to the NLO susceptibility $d^{-2\omega';\omega',\omega'}_{kij}$ measured at optical frequencies

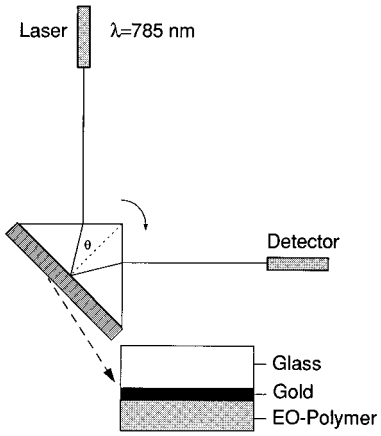

Figure 2. Schematic representation of the experimental ATR setup for the investigation of linear optical properties.

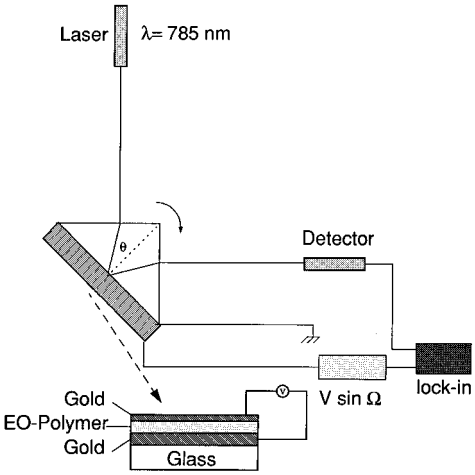

Figure 3. Schematic representation of the experimental ATR setup for the investigation of electro-optical properties.

ω' by

$$d_{ijk}^{\mathrm{EO}} \equiv d_{ijk}^{-2\omega';\omega',0} = \frac{f_i^{\omega} f_j^{\omega} f_k^{0}}{f_k^{2\omega'} f_i^{\omega'} f_j^{\omega'}} \frac{(3\omega_0^2 - \omega^2)(\omega_0^2 - \omega'^2)^2(\omega_0^2 - 4\omega'^2)}{(3\omega_0^2 - 3\omega'^2)(\omega_0^2 - \omega^2)^2\omega_0^2} d_{kij}^{-2\omega';\omega',\omega'} \quad (8)$$

III. Results and Discussion

Samples. The polymer investigated here is poly{[2-[2-(4-(dimethylamino)phenyl)vinyl]-5-nitro-1,4-phenylene]iminocarbonyldodecamethylenecarbonylimino} (**P12**) (T_g = 125 °C, x = 12 methylene units [see Figure 1]). Synthesis and characterization of this polymer have been reported previously, including linear and nonlinear optical measurements.[2,3] The sample preparation is described in the Experimental Section.

Measurements. In order to *directly* investigate the behavior of this NLO polymide in actual devices, the electro-optical properties of planar waveguides have been investigated by measurements of the waveguiding modes of such devices using attenuated-total-reflectance (ATR) spectroscopy.[7−9,31] This technique is an adequate tool to simultaneously measure birefringence and both non-zero electro-optical coefficients of a polymeric material and, hence, to also investigate the degree of order achieved by the poling process.

The experimental setups used are shown schematically in Figures 2 and 3; a full set of experiments for

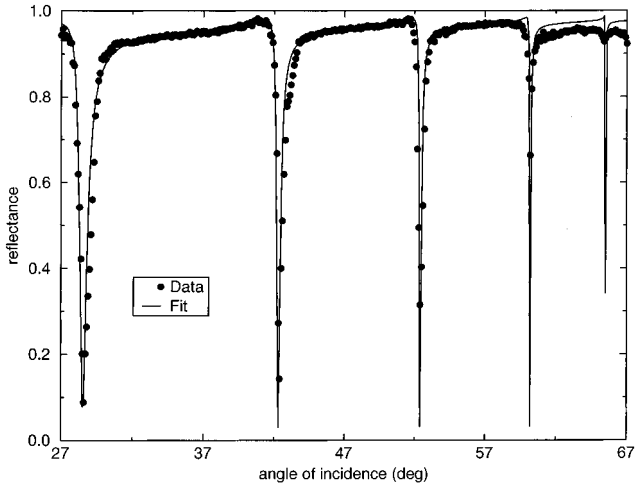

Figure 4. Reflected intensity as a function of the angle of incidence for TE polarized light, measured on a poled sample of $\mathbf{P_{12}}$ using the apparatus represented in Figure 2. Circles refer to measured data, while the solid line is the theoretical fit.

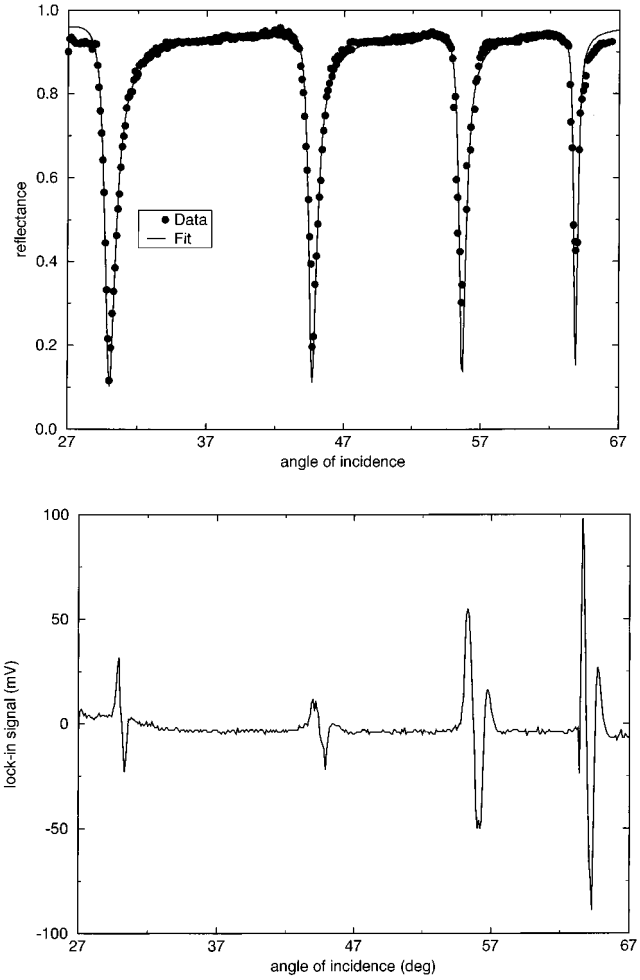

Figure 5. Reflected intensity (a) and a lock-in signal (b) as a function of the angle of incidence for TM polarized light, measured on a poled sample of $\mathbf{P_{12}}$ using the setup shown in Figure 3. A sinusoidal modulation (amplitude 1 V, 1 kHz) was applied to the device. Circles refer to measured data, while the solid line is the theoretical fit.

the same poled sample of **P12** is represented in Figures 4 and 5. The characterization of *linear* optical properties was performed with the setup shown in Figure 2. If a laser beam enters the prism at an angle that is sufficient for total internal reflection at the prism base,

an evanescent light field penetrates the gold, the thickness of which was adjusted to optimize the coupling. At certain angles of incidence, the in-plane propagation vector matches that of a waveguide mode, giving rise to a substantial drop in the reflected intensity, which, hereafter, is referred to as "dip". Figure 4 shows the reflected intensity as a function of the angle of incidence for TE polarized light. From these waveguide spectra, the thickness and the refractive indices of the polymeric layer could be determined, the latter with a relative accuracy of approximately 10^{-3}, by fitting the experimental spectra with Fresnel's formulas according to the procedures given by Swalen[32] and Zhang and Sasaki.[33]

The electro-optic effect in the waveguides was measured using the setup shown in Figure 3, by evaluating the influence of an electric field over the EO polymer (applied by the two gold electrodes) on the position of the dips. Since typical electro-optical coefficients are of the order of several picometers per volt, the relative changes in the refractive index that must be resolved are on the order of 10^{-3}. These subtle changes can, however, be easily observed with a modulation technique.[7,31,34] A sine wave of 1 V in amplitude at a frequency of 1 kHz was applied to the EO device. The modulation of the reflected intensity was recorded with a lock-in amplifier, operating at the fundamental frequency. At angles of incidence close to one of the mode dips, lock-in signals with a large signal-to-noise ratio were obtained, as is shown in Figure 5 for TM polarized light. The signal is proportional to the first derivative of the reflected intensity. This is expected if the modes are shifted by the field-induced changes in the refractive index of the waveguide.[35] The amplitude of the lock-in signal at the resonance angle permitted the determination of the electro-optic coefficients r_{13} and r_{33} of the EO waveguide using the methods described in detail before.[7−9] In the vicinity of a resonance, the first derivative of the ATR spectrum and the measured lock-in curves are proportional to each other and their ratio yields the field-induced angular shift of the respective resonance, independent of its width. The evaluation of the electro-optic coefficients from these shifts is then straightforward. In the first step we calculated the partial derivatives of the theoretical ATR curve with respect to the various parameters (i.e. refractive indices and thicknesses). This yielded, for every parameter separately, an "artificial lock-in signal" and thus, in a fashion similar to that for the measured signal, a set of theoretical values for the shifts of the mode dips. Fitting these sets of theoretical shifts to the set of the shifts measured, we finally obtained the field-induced changes on the refractive index by using the following formulas:[7]

$$r_{33} = \frac{2}{n^3_{\mathrm{TM}}} \frac{\partial n_{\mathrm{TM}}}{\partial F} \tag{9}$$

$$r_{13} = \frac{2}{n^3_{\mathrm{TE}}} \frac{\partial n_{\mathrm{TE}}}{\partial F} \tag{10}$$

where F denotes the electric field strength.

The photophysical properties of **P12** that have been measured are summarized in Table 1 and Figure 6, together with other relevant photophysical data, measured earlier using a conventional Maker-fringe technique. The electro-optic coefficients r_{13} and r_{33} have been determined to be 3.9 and 12.1 pm/V in the case of best orientation, as obtained here. Using different poling conditions, i.e. varying the poling voltage, time, or the distance between the corona and sample, the degree of orientation of the NLO-phores can be influenced and, thus, various devices with different EO responses could be prepared. Figure 6 shows the electro-optic coefficients versus the square root of the birefringence ($n = n_{\mathrm{TE}} - n_{\mathrm{TM}}$) for a series of such devices, showing a linear behavior for the two tensor components r_{13} and r_{33} on the corresponding birefringence components. Evidently, these ratios are not influenced by the degree of orientation. The ratio of the slopes of these two linear functions (formed by the ratio for the two tensor components r_{13} and r_{33}) is 3.1, in excellent agreement with the predictions of eq 6.

Table 1. Photophysical Properties of P_{12} Films

n_{TE}[a]	n_{TM}[a]	r_{33} (pm/V)[a]	r_{13} (pm/V)[a]	d_{33} (pm/V)[b]	d_{13} (pm/V)[b]	r^e_{33} (pm/V)[c]	r^e_{13} (pm/V)[c]
1.667	1.599	12.1	3.9	40	13	16	5

[a] Values measured with ATR at 785.5 nm. [b] Determined by Maker-fringe experiments at 1542 nm, as described in ref 2. [c] Value calculated for 1300 nm from the Maker-fringe experiments according to ref 2.

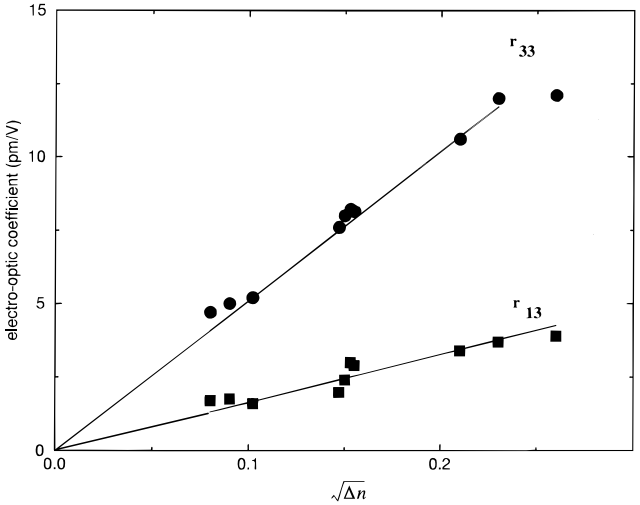

Figure 6. Electro-optical coefficients r_{13} and r_{33} as a function of the birefringence.

The experiments carried out on the waveguides prepared here, for the first time, show the suitability of the new NLO polyamides under investigation for the application in *actual devices*. The large electro-optic coefficients compare well with state-of-the-art EO polymers.[1] The EO coefficients, as directly measured here, are in accordance with the *electronic* EO coefficients that have been derived from the NLO susceptibilities[2] using relations 7 and 8. The values obtained using ATR spectroscopy are about 20% smaller than the values calculated from Maker-fringe experiments. Considering the different techniques used, especially bearing in mind the rather crude model which relates *electronic* EO and NLO coefficients[30] and the fact that the poling conditions that control the extent of NLO-phore orientation are difficult to reproduce exactly,[7,36] this deviation is surprisingly small.

The orientational behavior of the polymer **P_{12}** is in agreement with the predictions made by the *isotropic model*. First, as already discussed above, the average ratio of the EO coefficients r_{13} and r_{33} of 3.1 is in excellent accordance with the predictions of the model. The second concordance is the linear dependence of both electro-optic coefficients on the square root of the

birefringence. This behavior is expected in a first-order approximation for small poling parameters u (based on the static dipole moment of about 9 D of the NLO-phore DDANS[36] which the polymer investigated comprises and the poling fields of below 15 kV, the poling parameter u was estimated as significantly smaller than unity), since it has been shown that within the frame of this model the birefringence Δn must be proportional to u^2, while the electro-optic coefficients are proportional to u.[35]

The fact that the experimental results obtained using ATR spectroscopy are in good agreement with the *isotropic model* makes it evident that the NLO polymers based on DDANS discussed here are well described by the assumptions discussed in the theoretical section: Even after poling, the polymer samples are still completely amorphous (no aggregation or crystallinity present). Despite the fact that the NLO-phores are restricted in their mobility because they are rather rigidly incorporated into the polymer backbone, they behave like independent guest molecules dissolved in a polymer host. The attenuation in the device, due to optical absorption, is negligible at a wavelength (785.5 nm) that represents a regime interesting for various applications.[1]

IV. Conclusions

We recently proposed a new approach to the design of NLO polymers with large and extraordinarily stable second-order nonlinear susceptibilities, where the NLO-phores are part of the polymer backbone with their dipole moments oriented transversely to the polymer main chain.

In order to demonstrate the usefulness of these new NLO polyamides in actual devices, we investigated the electro-optical properties of planar waveguides by measurements of the waveguiding modes of these devices. Indeed, the results obtained using attenuated total reflectance spectroscopy prove the suitability of these materials for electro-optic applications. The electro-optic coefficient r_{33} of 12 pm/V compares favorably with state-of-the-art polymeric electro-optic materials. It also equals approximately the electronic contribution to the electro-optic effect as calculated from the nonlinear optical susceptibility d_{33}. The ratio of electro-optic coefficients r_{33} and r_{31} was found to be independent of the magnitude of the NLO-phore orientation and equal to 3. This behavior is in perfect agreement with the predictions from the *isotropic model*.

V. Experimental Section

Materials. Synthesis and characterization of the polymer used in this work (poly{[2-[2-(4-(dimethyamino)phenyl)vinyl]-5-nitro-1,4-phenylene]iminocarbonyldodecamethylene-carbonylimino}, $\mathbf{P}_{12}$, T_g = 125 °C, 12 methylene units [see Figure 1]) have been described previously.[2]

Device Preparation. The polymer was dissolved in dry NMP at concentrations of 4−8% w/w. The solutions were filtered through a 0.45 μm Teflon filter and were spin-cast onto slides of high-refractive-index glass (n = 1.80) that were previously covered by a gold layer (Balzers 99.99%) of approximately 30−40 nm thickness. The samples were dried at 70 °C in vacuum for at least 24 h. The thickness of the polymer films ranged from 0.5 to 1.5 μm. The samples were corona poled with a dc electric field using a custom-made hotstage as the ground electrode and a tungsten corona needle. The applied corona voltage was up to +15 kV at a gap distance of approximately 3 cm. The films were heated under an applied field to 5−15 deg above T_g, held at this temperature for about 30 min, and then cooled to room temperature at an average rate of 1.5−3 °C/min. These samples were used for the determination of the linear optical properties, as discussed below. For the measurement of the electro-optic response, a top layer of gold of approximately 100 nm thickness was thermally evaporated subsequently onto these devices. In order to obtain multiple, independent devices on a single polymer film, the gold electrodes were applied in well-defined patterns, as sketched in Figure 7. The active area of these devices was 16 mm^2.

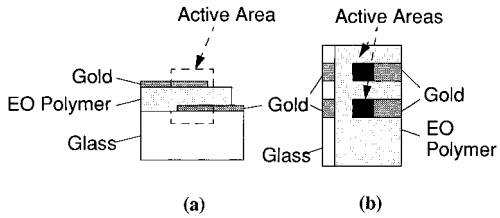

Figure 7. Schematic representation of the device employed: (a) front view; (b) top view.

ATR Experiment. The experimental setups used are sketched in Figures 2 and 3. A diode laser working at a frequency of 785.5 nm and a power of 5 mW was used as the light source (Hitachi HL7806G). The light was polarized to TM or TE by means of a rotating polarizer and focused with conventional optics to the base of the prism. The laser was mounted on a computer-controlled, stepping motor driven (C-560, Physik Instrumente) translation stage, in order to adjust the laser spot throughout the experiment to the center of the prism base (it is of extreme importance to ensure that the entire experiment is performed on exactly the same section of the device). The material of the prism was identical to the substrates used. The glass slide upon which the waveguiding device had been prepared was attached to the prism with an index matching fluid (n = 1.8, Cargille Laboratories Inc., Cedar Grove, NJ). The prism was mounted on a rotating stage, which was also driven by a computer-controlled stepping motor that allowed an angular step size of 10^{-3} °. A silicon photodiode (Temic BPW 20R) with a maximum sensitivity at 750 nm was used as the detector. It was fitted with a focusing lens, a diaphragm that allowed us to only detect the light in the center of the spot (1.5 mm diameter), an analyzer, and a filter (with a cutoff at around 650 nm) to reduce the effect of adventitious light. The detector was mounted on a goniometer, which was also driven by a computer-controlled stepping motor that allowed us to follow the reflected light. The system was calibrated so as to ensure the optical alignment of the major components (laser−prism base−detector) throughout an experiment.

Acknowledgment. Financial support by the Schweizerischer Nationalfonds zur Förderung der wissenschaftlichen Forschung (NF Sektion II) is gratefully acknowledged. The authors thank J. Roth for the development of the software to control the experimental setups used.

References and Notes

(1) See for example: *Nonlinear Optical and Electroactive Polymers*; Prasad, P. N., Ulrich, D. R., Eds.; Plenum Press: New York, 1988. Lytel, R.; Lipscomb, G. F.; Kenney, J. T.; Binkley, E. S. In *Polymers for Lightwave and Integrated Optics*; Hornack, L. A., Ed.; Marcel Dekker: New York, 1992. Papers presented in *Organic Thin Films for Photonic Applications*; Technical Digest Series Vol. 17; Optical Society of America: Washington, DC, 1993.

(2) Weder, Ch.; Neuenschwander, P.; Suter, U. W.; Prêtre, P.; Kaatz, P.; Günter, P. *Macromolecules* **1994**, *27*, 2181.

(3) Weder, Ch.; Neuenschwander, P.; Suter, U. W.; Prêtre, P.; Kaatz, P.; Günter, P. *Macromolecules* **1995**, *28*, 2377.

(4) Weder, Ch.; Glomm, B. H.; Neuenschwander, P.; Suter, U. W. *Macromol. Chem. Phys.* **1995**, *196*, 1113.

(5) Weder, Ch.; Neuenschwander, P.; Suter, U. W.; Prêtre, P.; Kaatz, P.; Günter, P. *Mol. Cryst. Liq. Cryst. Sci. Technol., Sect B* **1996**, *15*, 395.

(6) Lang, F. R.; Franzreb, K.; Pitton, Y.; Xanthopoulos, N.; Landolt, D.; Mathieu, H. J.; Döbler, M.; Weder, Ch.; Neuenschwander, P.; Suter, U. W. Proceedings of the 6th European Conference on Application of Surface and Interface Analysis, ECASIA, Montreux, Switzerland, 1995.
(7) Herminghaus, S.; Smith, B. A.; Swalen, J. D. *J. Opt. Soc. Am. B* **1991**, *8*, 2311.
(8) Herminghaus, S.; Boese, D.; Yoon, D. Y.; Smith, B. A. *Appl. Phys. Lett.* **1991**, *59*, 1043.
(9) Bolognesi, A.; Bajo, D.; Villa, D.; Ahumada, O. *Thin Solid Films*, in press.
(10) Williams, D. J. In *Nonlinear Optical Properties of Organic Molecules and Crystals*; Chemla, D. S., Zyss, J., Eds.; Academic Press: New York, **1987**; Vol. 1, p 405.
(11) Burland, D. M.; Miller, R. D.; Walsh, C. A. *Chem. Rev.* **1994**, *94*, 31.
(12) Williams, D. In *Electronic and Photonic Applications of Polymers*; Bowden, M. J., Turner, S. R., Eds.; *Advances in Chemistry Series*; American Chemical Society: Washington, DC, 1988; No. 218, p 317.
(13) Singer, K. D.; Kuzyk, M. G.; Sohn, J. E. *J. Opt. Soc. Am. B* **1987**, *4*, 968.
(14) Page, R.; Jurich, M.; Reck, B.; Sen, A.; Twieg, R.; Swalen, J. D.; Bjorklund, G.; Willson, C. *J. Opt. Soc. Am. B* **1990**, *7*, 1239.
(15) Wijekoon, W.; Zhang, Y.; Karna, S.; Prasad, P. Griffin, A.; Bhatti, A. *J. Opt. Soc. Am. B* **1992**, *9*, 1832.
(16) Abramowitz, M.; Stegun, I. *Handbook of Mathematical Functions with Formulas, Graphs and Mathematical Table*; Dover: New York, 1965.
(17) Zyss, J.; Oudar, J. L. *Phys. Rev.* **1982**, *A26*, 2028.
(18) Kleinman, D. A. *Phys. Rev.* **1962**, 126, 1977.
(19) Singer, K.; Kuzyk, M.; Sohn, J. *J. Opt. Soc. Am. B* **1987**, *4*, 968.
(20) Eich, M.; Bjorklund, G. C.; Yoon, D. Y. *Polym. Adv. Technol.* **1990**, *1*, 189.
(21) Jungbauer, D.; Reck, B.; Twieg, R.; Yoon. D.; Willson, C.; Swalen, J. D. *J. Appl. Phys. Lett.* **1990**, *56*, 2610.
(22) Boyd, G.; Francis, C.; Trend, J.; Ender, D. *J. Opt. Soc. Am. B* **1991**, *8*, 887.
(23) Jeng, R.; Chen, Y. M.; Jain, A. K.; Tripathy, S. K.; Kumar, J. *Opt. Commun.* **1992**, *89*, 212.
(24) Yitzchaik, S.; Berkovic, G.; Kronganz, V. *Macromolecules* **1990**, *23*, 3541.
(25) Eich, M.; Looser, H.; Yoon, D.; Twieg, R.; Bjorklund, G.; Baumert, J. *J. Opt. Soc. Am. B* **1989**, *6*, 1590.
(26) Meyreix, R.; Lecomte, J.; Tapolsky, G. *Nonlinear Opt.* **1991**, *1*, 201.
(27) Amano, M.; Kainoo, T.; Yamamoto, F.; Takenchi, Y. *Mol. Cryst. Liq. Cryst.* **1990**, *182 A*, 81.
(28) Skumanich, A.; Jurich, M.; Swalen, J. *Appl. Phys. Lett.* **1993**, *62*, 446.
(29) Bosshard, Ch.; Sutter, K.; Pretre, Ph.; Hulliger, J.; Florsheimer, M.; Kaatz, P.; Günter, P. *Organic Nonlinear Optical Materials*; Advances in Nonlinear Optics Vol 1; Gordon and Breach Publishers: New York, **1995**. There are, however, certain exceptions; see: Herminghaus, S.; Conradt, R.; Aust, E.; Knoll, W.; Takahashi,Y.; Ukishima, S.; Fukada, E.; Boese, D. *Opt. Commun.* **1996**, *123*, 250.
(30) Boyd, G. D.; Kleinman, D. A. *J. Appl. Phys.* **1968**, *39*, 3597.
(31) Dentan, V.; Levy, Y.; Dumont, M.; Robin, P.; Chastaing, E. *Opt. Commun.* **1989**, *69*, 379.
(32) Swalen, J. D. *J. Mol. Electron.* **1986**, *2*, 155.
(33) Zhang, G.; Sasaki, K. *Appl. Opt.* **1988**, *27*, 1358.
(34) Dentan, V.; Levy, Y.; Morichere, D. Electrooptic Organic Waveguides: Optical Characterization. In *Proceedings of the NATO Conference on Organic Molecules for Nonlinear Optics and Photonics*; Messier, S., Ed.; Kluwer Academic, Norwell, MA, **1990**; p 461.
(35) Page, R.; Jurich, M.; Reck, B.; Sen, A.; Twieg, R.; Swalen, J.; Bjorklund, G.; Willson, C. *J. Opt. Soc. Am. B* **1990**, *7*, 1239.
(36) Weder, Ch. Ph.D. thesis No. 10749, ETH Zürich, 1994.

MA9618989